Robust-Adaptive Two-Loop Control for Robots with Mixed Rigid-Elastic Joints

Minh Tuan Hua[1*], Emil Mühlbradt Sveen[1], Siri Marte Schlanbusch[1], Filippo Sanfilippo[1]

Abstract— **In robotics, while rigid joints are common due to their accuracy and fast response ability, elastic joints are well-known for their safety when interacting with the environment. To harmonise the advantages of these joint types, robots with mixed rigid-elastic joints can be considered. In this paper, a robust-adaptive two-loop control algorithm is proposed to control this type of hybrid robots when there are uncertainties in system parameters. In the outer loop, a robust control algorithm is proposed to deal with the uncertainties in the parameters of the joint dynamics, together with an adaptive controller for the rigid joints. In the inner loop, another robust control algorithm is proposed to handle the uncertainties in system parameters of the elastic joint's motor contribution, and a similar adaptive control algorithm is presented to manipulate the elastic joints' motors. The stability of the system is assured by Lyapunov's stability theory. Finally, simulations are conducted to verify the proposed control algorithm.**

I. INTRODUCTION

In industrial robots, rigid joints are popular for their strength, high accuracy in position control, and fast response time [1], [2]. However, they often operate in isolated workspaces due to the excessive interaction forces they generate, which can cause harm. In contrast, collaborative robots, which interact closely with humans, typically use elastic joints for their safety. These joints, however, have poorer accuracy and slower response times compared to rigid joints [1], [2]. To leverage the advantages and mitigate the drawbacks of both joint types, robots with mixed joints can be used. Figure 1 illustrates such a robot, used later in the simulation section. This robot has six degrees of freedom, with the first three joints being rigid and the last three elastic.

Various works on controlling robots with elastic joints have been presented in the literature [3]. The dynamic model of robots with elastic joints can be considered in complete [4], [5] or reduced form [6]. In [7], a practical robust controller is proposed, consisting of model-based computed torque control, feedback-based control, and robust control. The efficiency of this control algorithm is verified through simulations against inertia and stiffness uncertainties. In [8], a terminal sliding mode control (TSMC) with a cascaded finite-time sliding mode observer (CFTSMO) is presented for the robots with flexible joints to ensure the finite-time convergence of the system output and to obtain the robustness against the lumped disturbance and estimation error. In [9], a chattering-suppressed sliding mode controller is introduced. A radial basis function neural network (RBFNN) based soft computing strategy is presented to reduce the chattering in the sliding mode controller. In addition, an extended Kalman filter is designed to facilitate the closed-loop tracking control without position or velocity measurements of links. In [10], a nonlinear disturbance observer (NDOB)-based robust controller is investigated for multi-joint series elastic actuator (SEA)-driven robots. A fast-time control signal is designed according to the singular perturbation theory to stabilise the SEA-level dynamics. Then, an NDOB is combined with a computed torque controller to achieve a composite controller.

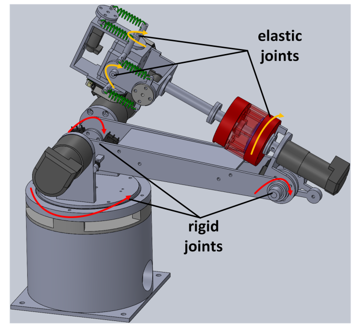

Fig. 1. The adopted hybrid rigid-elastic robot. For rigid joints, motors and joints are connected rigidly through gearboxes. For elastic joints, motors and joints are coupled via elastic elements (springs in the robot shown).

Adaptive controllers are used to address uncertainties in system parameters for robots with elastic joints. In [11], an extended state observer (ESO) estimates the velocity states and joint stiffness uncertainties of a flexible-joint manipulator, followed by an adaptive backstepping controller based on a new state-space representation of the dynamic model. In [12], a novel neural adaptive controller is introduced, using a network to approximate the robot dynamics in a linear-in-parameter form. The output layer weights are updated rapidly using a Lyapunov-based adaptation law, while the internal weights are updated slowly through online back-propagation. In [13], an adaptive fuzzy global coupled nonsingular fast terminal sliding mode control (NFTSMC) is proposed for robots with elastic joints, addressing uncertainties. This fuzzy approximator eliminates singularity, improves tracking speed, and reduces chattering effects. In [14], an inverse optimal adaptive neural control algorithm is presented, where the inverse optimal controller is updated using a tuning functions-based adaptive learning technique. This approach ensures that the number of learning parameters remains independent of the robot's link count and the dimension

This research is supported by the Artificial Intelligence, Biomechatronics, and Collaborative Robotics research group at the Top Research Center Mechatronics (TRCM), University of Agder (UiA), Norway.

[1]The authors are with the Department of Engineering Sciences, Faculty of Engineering and Science, University of Agder, Jon Lilletuns vei 9, 4879 Grimstad.

[*]minh.tuan.hua@uia.no

of the neural optimal weight vector. In [15], a two-loop control scheme is proposed. The inner control loop is a model reference adaptive controller (MRAC) to handle uncertainties in the system parameters. The outer control loop adopts a fuzzy proportional-integral control mechanism to reduce the effect of external disturbances on the load.

To the best of the authors' knowledge, only a few works related to robots with mixed rigid-elastic joints exist. In [4], [5], a decoupling and linearisation for robots with mixed joint types via dynamic feedback is introduced. A linear dynamic feedback compensator for the inputs at the rigid joints to imitate the behaviour of the elastic joints is designed. However, the algorithm requires high order of derivatives of the desired and actual position of the joints. In [16], [17], an adaptive control algorithm based on the virtual decomposition method for mixed rigid-flexible joint manipulators is considered. Yet, it is required to estimate many parameters, including the mass, centre of mass, and inertia of the links [18].

In this paper, a novel robust-adaptive two-loop control algorithm is introduced to control a robot with mixed rigid-elastic joints. The dynamics of the robot is separated into two parts: the joint dynamics, and the contribution related to the motor of the elastic joints. The joint dynamics describes the dynamic relationship between the joint velocities, accelerations, and torques. The joint torques are constituted of the motor torques from the rigid joints and the elastic torques from the elastic joints. The contribution related to the motor of the elastic joints describes the dynamic relationship between the velocities, accelerations, and torques. The joint dynamics is controlled in the outer loop, while the part concerning the motor of the elastic joints is controlled in the inner loop of the proposed algorithm. In particular, in the outer loop, a robust control algorithm based on computed torque [18] is presented to compensate for the uncertainties in the dynamic parameters of the joint dynamics. Then, for rigid joints, an adaptive control algorithm [19] is developed, and its output signal is added to the output of the robust control algorithm. For the elastic joints, the outputs of the robust control algorithm are used to calculate the desired motor positions. In the inner loop, a robust control algorithm also based on computed torque is proposed to tackle the uncertainties in the system parameters on the elastic joint's motor side. Successively, an adaptive control algorithm is designed and then added to the output of the robust control algorithm to control the elastic joint motors. The stability of the proposed robust-adaptive two-loop control algorithm is ensured by Lyapunov's stability theory. The proposed control method has the advantage of addressing fast-changing disturbances with high-gain robust and computed torque controllers, allowing adaptive controllers to handle only slow-changing uncertainties. For each joint, the adaptive controller estimates just two parameters: motor inertia around the rotational axis and the sum of the friction coefficient and back electromotive force coefficient. The efficiency of the control algorithm is confirmed through simulations.

This paper is organised as follows. In Section II, the dynamic model of robots with mixed rigid-elastic joints is summarised. Then, in Section III, the proposed robust-adaptive two-loop control algorithm is designed. In Section IV, simulations are presented. Finally, the conclusions are presented in Section V.

II. DYNAMIC MODEL

Consider a robot with N joints, where there are $N_e < N$ elastic joints, and $N_r = N - N_e$ rigid joints. The following assumptions are made for the dynamic model of the considered robot:

Assumption 1: the elasticity region is limited in the linear elasticity region, where the Hooke's law is applicable.

Assumption 2: the motors are modelled as uniform bodies with their centres of mass on the rotation axis.

Assumption 3: only rotary electric motors are considered. Other types of actuators, such as hydraulic and pneumatic actuators are out of the scope of this work.

Let $\mathbf{q} = [q_1 \ q_2 \ ... \ q_N]^T$ and $\boldsymbol{\theta} = [\theta_1 \ \theta_2 \ ... \ \theta_{N_e}]^T$ denote the vector of joint variables and the vector of motor angular positions of the elastic joints, respectively. Note that θ_k is the angular position of the motor of the k^{th} elastic joint corresponding to joint i. For example, if a robot has three joints, where the last one is an elastic joint, then θ_1 controls q_3. For easy reading, they will be denoted as $\theta_{k,i}$. Let $\boldsymbol{M}(\mathbf{q}) = \boldsymbol{M}_{JC}(\mathbf{q}) + \boldsymbol{M}_I$ denote the mass matrix of the robot, where it is decomposed into $\boldsymbol{M}_{JC}$ containing the Jacobian matrices and coupling components and the diagonal matrix $\boldsymbol{M}_I = diag(M_{I_1}, M_{I_2}, ..., M_{I_N})$ containing the inertia of motors I_{mz_i} of the rigid joints around their rotational axes, and:

$$M_{I_i} = \begin{cases} 0 & \text{if joint } i \text{ is an elastic joint} \\ {\eta_{m_i}}^2 I_{mz_i} & \text{if joint } i \text{ is a rigid joint} \end{cases} \quad (1)$$

where η_{m_i} is the gear ratio of motor i. Let $\boldsymbol{B}$ denote the diagonal matrix containing the inertia of motors of the elastic joints around their rotational axes. Let $\boldsymbol{S}(\mathbf{q})$, $\boldsymbol{C}(\mathbf{q}, \dot{\mathbf{q}})$, $\boldsymbol{C}_1(\mathbf{q}, \dot{\mathbf{q}})$, and $\boldsymbol{C}_2(\mathbf{q}, \dot{\mathbf{q}})$ denote the coupling matrix between the rigid and elastic joints, and the matrices of Coriolis and centrifugal forces, respectively. Let $\mathbf{G}(\mathbf{q})$ denote the vector of gravitational forces. Define a dynamic vector as below:

$$\boldsymbol{\xi}(\mathbf{q}, \dot{\mathbf{q}}, \dot{\boldsymbol{\theta}}, \ddot{\boldsymbol{\theta}}) = \boldsymbol{S}(\mathbf{q})\ddot{\boldsymbol{\theta}} + \boldsymbol{C}_1(\mathbf{q}, \dot{\mathbf{q}})\dot{\boldsymbol{\theta}} + \mathbf{G}(\mathbf{q}) \quad (2)$$

Let $\boldsymbol{\mu}_{mr}^v$ denote the diagonal matrix of friction coefficients, $\boldsymbol{\tau}_{mr}$ symbolise the vector of motor torques, and $\boldsymbol{\tau}_{elas}^q$ express the vector of elastic torques of the joint dynamics:

$$\boldsymbol{\mu}_{mr}^v = \text{diag}(\mu_{mr_1}^v, \mu_{mr_2}^v, ..., \mu_{mr_N}^v), \quad (3)$$
$$\mu_{mr_i}^v = \begin{cases} 0 & \text{if joint } i \text{ is an elastic joint} \\ \mu_{m_i}^v & \text{if joint } i \text{ is a rigid joint} \end{cases}$$

$$\boldsymbol{\tau}_{mr} = [\tau_{mr_1} \ \tau_{mr_2} \ ... \ \tau_{mr_N}]^T, \quad (4)$$
$$\tau_{mr_i} = \begin{cases} 0 & \text{if the joint } i \text{ is an elastic joint} \\ \tau_{m_i}(t) & \text{if the joint } i \text{ is a rigid joint} \end{cases}$$

$$\boldsymbol{\tau}^q_{elas} = [\tau^q_{elas_1}\ \tau^q_{elas_2}\ ...\ \tau^q_{elas_N}]^T, \tag{5}$$
$$\tau^q_{elas_i} = \begin{cases} K_{k,i}(\theta_{k,i} - q_i) & \text{if joint } i \text{ is the } k^{th} \text{ elastic joint} \\ 0 & \text{if joint } i \text{ is a rigid joint} \end{cases}$$

where $K_{k,i}$ is the stiffness of the k^{th} elastic joint. $\boldsymbol{\mu}^v_{me}$, $\boldsymbol{\tau}_{me}$, and $\boldsymbol{\tau}_{elas}$ are these quantities of the elastic joint's motor contribution.

Consider the dynamic equations of a robot with mixed rigid-elastic joints [4], [5]:

$$\begin{cases} \boldsymbol{M}_{JC}(\mathbf{q})\ddot{\mathbf{q}} + \boldsymbol{C}(\mathbf{q}, \dot{\mathbf{q}})\dot{\mathbf{q}} + \boldsymbol{\xi}(\mathbf{q}, \dot{\mathbf{q}}, \dot{\boldsymbol{\theta}}, \ddot{\boldsymbol{\theta}}) \\ \qquad + \boldsymbol{M}_I\ddot{\mathbf{q}} + \boldsymbol{\mu}^v_{mr}\dot{\mathbf{q}} = \boldsymbol{\tau}_{mr} + \boldsymbol{\tau}^q_{elas} \\ \boldsymbol{S}(\mathbf{q})^T\ddot{\mathbf{q}} + \boldsymbol{C}_2(\mathbf{q}, \dot{\mathbf{q}})\dot{\mathbf{q}} + \boldsymbol{\tau}_{elas} + \boldsymbol{B}\ddot{\boldsymbol{\theta}} + \boldsymbol{\mu}^v_{me}\dot{\boldsymbol{\theta}} = \boldsymbol{\tau}_{me} \end{cases} \tag{6}$$

Assuming that the joints are driven by DC motors. Let R_{a_i}, K_{τ_i}, K_{emf_i}, w_{m_i}, and v_{c_i} denote the armature resistance, torque coefficient, back electromotive force coefficient, rotational velocity, and the control voltage of motor i, respectively. The equation presents the mechanical-electrical relationship of motor i is [20]:

$$\tau_{m_i} = \eta_{m_i}\frac{K_{\tau_i}}{R_{a_i}}(v_{c_i} - K_{emf_i}\eta_{m_i}w_{m_i}) = K_{t_i}v_{c_i} - K_{e_i}w_{m_i} \tag{7}$$

where

$$K_{t_i} = \eta_{m_i}\frac{K_{\tau_i}}{R_{a_i}},\ K_{e_i} = \eta^2_{m_i}\frac{K_{\tau_i}K_{emf_i}}{R_{a_i}} \tag{8}$$

Let $\boldsymbol{K}_{tr}$, $\boldsymbol{K}_{er}$, $\mathbf{v}_{cr}$, $\boldsymbol{K}_{te}$, $\boldsymbol{K}_{ee}$, and $\mathbf{v}_{ce}$ denote the diagonal matrices collecting the K_{t_i} constants, the diagonal matrices collecting the K_{e_i} constants, and the vector collecting control voltages of the rigid and elastic joints, respectively, where:

$$\boldsymbol{K}_{tr} = \text{diag}(K_{tr_1}, K_{tr_2}, ..., K_{tr_N}), \tag{9}$$
$$K_{tr_i} = \begin{cases} 1 & \text{if joint } i \text{ is an elastic joint} \\ K_{t_i} & \text{if joint } i \text{ is a rigid joint} \end{cases}$$

$$\boldsymbol{K}_{er} = \text{diag}(K_{er_1}, K_{er_2}, ..., K_{er_N}), \tag{10}$$
$$K_{er_i} = \begin{cases} 0 & \text{if joint } i \text{ is an elastic joint} \\ K_{e_i} & \text{if joint } i \text{ is a rigid joint} \end{cases}$$

$$\mathbf{v}_{cr} = [v_{cr_1}\ v_{cr_2}\ ...\ v_{cr_N}]^T, \tag{11}$$
$$v_{cr_i} = \begin{cases} 0 & \text{if joint } i \text{ is an elastic joint} \\ v_{c_i} & \text{if joint } i \text{ is a rigid joint} \end{cases}$$

Let $\boldsymbol{K}_{te}$, $\boldsymbol{K}_{ee}$, and $\mathbf{v}_{ce}$ denote these matrices and vector for elastic joints, where

$$\begin{aligned} \boldsymbol{K}_{te} &= \text{diag}(K_{te_1}, K_{te_2}, ..., K_{te_{N_e}}) \\ \boldsymbol{K}_{ee} &= \text{diag}(K_{ee_1}, K_{ee_2}, ..., K_{ee_{N_e}}) \\ \mathbf{v}_{ce} &= [v_{ce_1}\ v_{ce_2}\ ...\ v_{ce_{N_e}}]^T \end{aligned} \tag{12}$$

where $K_{te_k} = K_{t_i}$, $K_{ee_k} = K_{e_i}$, and $v_{ce_k} = v_{c_i}$ if joint i is the k^{th} elastic joint. Then:

$$\boldsymbol{\tau}_{mr} = \boldsymbol{K}_{tr}\mathbf{v}_{cr} - \boldsymbol{K}_{er}\dot{\mathbf{q}},\quad \boldsymbol{\tau}_{me} = \boldsymbol{K}_{te}\mathbf{v}_{ce} - \boldsymbol{K}_{ee}\dot{\boldsymbol{\theta}} \tag{13}$$

Let $\boldsymbol{\mu}^{di}_{mr} = \boldsymbol{\mu}^v_{mr} + \boldsymbol{K}_{er}$ and $\boldsymbol{\mu}^{di}_{me} = \boldsymbol{\mu}^v_{me} + \boldsymbol{K}_{ee}$ denote the disturbances coefficient matrices of the rigid and elastic joints, respectively. Let q_{d_i} and $\theta_{d_{k,i}}$ denote the desired position of joint i and the desired motor position of the k^{th} elastic joint, respectively. Let $\mathbf{q}_d$ and $\boldsymbol{\theta}_d$ denote the vector collecting the desired quantities. Let quantities with "$\hat{}$" above denote the nominal or estimated quantities. The desired elastic force $\hat{\boldsymbol{\tau}}^q_{elas}$ is defined as:

$$\hat{\boldsymbol{\tau}}^q_{elas} = [\hat{\tau}^q_{elas_1}\ \hat{\tau}^q_{elas_2}\ ...\ \hat{\tau}^q_{elas_N}]^T, \tag{14}$$
$$\hat{\tau}^q_{elas_i} = \begin{cases} \hat{K}_{k,i}(\theta_{d_{k,i}} - q_{d_i}) & \text{joint } i \text{ is the } k^{th} \text{ elastic joint} \\ 0 & \text{joint } i \text{ is a rigid joint} \end{cases}$$

Let $\tilde{\boldsymbol{\tau}}^q_{elas} = \hat{\boldsymbol{\tau}}^q_{elas} - \boldsymbol{\tau}^q_{elas}$ denote the error between desired and actual elastic forces. Because the elements in the matrix $\boldsymbol{K}_{tr}$ corresponding to the elastic joints equal to 1, then $\hat{\boldsymbol{\tau}}^q_{elas} = \boldsymbol{K}_{tr}\hat{\boldsymbol{\tau}}^q_{elas}$. Consequently, the dynamic equations (6) are rewritten as:

$$\begin{aligned} &\begin{cases} \boldsymbol{M}_{JC}(\mathbf{q})\ddot{\mathbf{q}} + \boldsymbol{C}(\mathbf{q}, \dot{\mathbf{q}})\dot{\mathbf{q}} + \boldsymbol{\xi}(\mathbf{q}, \dot{\mathbf{q}}, \dot{\boldsymbol{\theta}}, \ddot{\boldsymbol{\theta}}) \\ \qquad + \boldsymbol{M}_I\ddot{\mathbf{q}} + \boldsymbol{\mu}^v_{mr}\dot{\mathbf{q}} + \tilde{\boldsymbol{\tau}}^q_{elas} = \boldsymbol{K}_{tr}\mathbf{v}_{cr} - \boldsymbol{K}_{er}\dot{\mathbf{q}} + \hat{\boldsymbol{\tau}}^q_{elas} \\ \boldsymbol{S}(\mathbf{q})^T\ddot{\mathbf{q}} + \boldsymbol{C}_2(\mathbf{q}, \dot{\mathbf{q}})\dot{\mathbf{q}} + \boldsymbol{\tau}_{elas} + \boldsymbol{B}\ddot{\boldsymbol{\theta}} + \boldsymbol{\mu}^v_{me}\dot{\boldsymbol{\theta}} \\ \qquad = \boldsymbol{K}_{te}\mathbf{v}_{ce} - \boldsymbol{K}_{ee}\dot{\boldsymbol{\theta}} \end{cases} \\ \Leftrightarrow &\begin{cases} \boldsymbol{M}_{JC}(\mathbf{q})\ddot{\mathbf{q}} + \boldsymbol{C}(\mathbf{q}, \dot{\mathbf{q}})\dot{\mathbf{q}} + \boldsymbol{\xi}(\mathbf{q}, \dot{\mathbf{q}}, \dot{\boldsymbol{\theta}}, \ddot{\boldsymbol{\theta}}) \\ \qquad + \boldsymbol{M}_I\ddot{\mathbf{q}} + \boldsymbol{\mu}^{di}_{mr}\dot{\mathbf{q}} + \tilde{\boldsymbol{\tau}}^q_{elas} = \boldsymbol{K}_{tr}(\mathbf{v}_{cr} + \hat{\boldsymbol{\tau}}^q_{elas}) \\ \boldsymbol{S}(\mathbf{q})^T\ddot{\mathbf{q}} + \boldsymbol{C}_2(\mathbf{q}, \dot{\mathbf{q}})\dot{\mathbf{q}} + \boldsymbol{\tau}_{elas} + \boldsymbol{B}\ddot{\boldsymbol{\theta}} + \boldsymbol{\mu}^{di}_{me}\dot{\boldsymbol{\theta}} = \boldsymbol{K}_{te}\mathbf{v}_{ce} \end{cases} \end{aligned} \tag{15}$$

III. ROBUST-ADAPTIVE TWO-LOOP CONTROLLER

A. Design specifications

The design specification for robust control is to ensure the robustness against the uncertainties in system parameters. Regarding the adaptive control, the goal is to learn the inertia of the motor around the rotational axis, and the cumulative contribution of the friction coefficient with the back electromotive force coefficient, which are the disturbances coefficient matrices of the rigid and elastic joints, $\boldsymbol{\mu}^{di}_{mr}$ and $\boldsymbol{\mu}^{di}_{me}$, respectively.

B. Control signal for the joint dynamics

Figure 2 illustrates the proposed robust-adaptive two-loop control algorithm. Consider the control law for the joint dynamics consisting of three parts, namely the computed torque control part $\mathbf{u}^{ct}_q$, the tracking control $\mathbf{u}^{tr}_q$, and the robust control part $\mathbf{u}^{ro}_q$:

$$\mathbf{v}_{cr} + \hat{\boldsymbol{\tau}}^q_{elas} = \mathbf{u}_q = \mathbf{u}^{ct}_q + \mathbf{u}^{tr}_q + \mathbf{u}^{ro}_q \tag{16}$$

The computed torque control part $\mathbf{u}^{ct}_q$ is utilised as a feed-forward control law to handle the nonlinearities on the joint dynamics, the tracking control part $\mathbf{u}^{tr}_q$ is proposed to manipulate the motors of rigid joints, and the robust control part $\mathbf{u}^{ro}_q$ is proposed to deal with the uncertainties on the joint dynamics. Furthermore, to cope with the uncertainties when manipulating the motors of rigid joints, an adaptation law is proposed. Let $\boldsymbol{K}_{Pq}$ and $\boldsymbol{K}_{Dq}$ denote the diagonal matrices

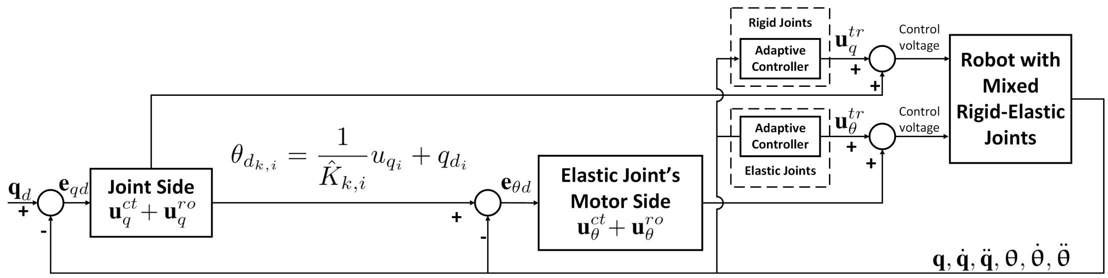

Fig. 2. The proposed robust-adaptive two-loop controller diagram.

with the PD control gains for the joint dynamics, respectively. Let $\mathbf{e}_{qd} = \mathbf{q}_d - \mathbf{q}$ denote the error vector. Consider the computed torque control law:

$$\mathbf{u}_q^{ct} = \hat{\boldsymbol{K}}_{tr}^{-1}(\hat{\boldsymbol{M}}_{JC}\ddot{\mathbf{q}}_d + \hat{\boldsymbol{C}}\dot{\mathbf{q}}_d + \hat{\boldsymbol{\xi}} + \boldsymbol{K}_{Pq}\mathbf{e}_{qd} + \boldsymbol{K}_{Dq}\dot{\mathbf{e}}_{qd}) \quad (17)$$

Substituting (17) into the dynamic equation of the joint dynamics in (15) gives:

$$\begin{aligned} &\boldsymbol{M}_I\ddot{\mathbf{q}} + \boldsymbol{\mu}_{mr}^{di}\dot{\mathbf{q}} = \boldsymbol{K}_{tr}(\mathbf{u}_q^{tr} + \mathbf{u}_q^{ro}) - \tilde{\boldsymbol{\tau}}_{elas}^q - \boldsymbol{K}_{tr}\boldsymbol{\delta}_q \\ &\quad + \boldsymbol{M}_{JC}\ddot{\mathbf{e}}_{qd} + (\boldsymbol{K}_{tr}\hat{\boldsymbol{K}}_{tr}^{-1}\boldsymbol{K}_{Dq} + \boldsymbol{C})\dot{\mathbf{e}}_{qd} + \boldsymbol{K}_{tr}\hat{\boldsymbol{K}}_{tr}^{-1}\boldsymbol{K}_{Pq}\mathbf{e}_{qd} \end{aligned} \quad (18)$$

where

$$\tilde{\boldsymbol{M}}_{JC} = \hat{\boldsymbol{K}}_{tr}^{-1}\hat{\boldsymbol{M}}_{JC} - \boldsymbol{K}_{tr}^{-1}\boldsymbol{M}_{JC}, \quad \tilde{\boldsymbol{C}} = \hat{\boldsymbol{K}}_{tr}^{-1}\hat{\boldsymbol{C}} - \boldsymbol{K}_{tr}^{-1}\boldsymbol{C} \quad (19)$$

$$\tilde{\boldsymbol{\xi}} = \hat{\boldsymbol{K}}_{tr}^{-1}\hat{\boldsymbol{\xi}} - \boldsymbol{K}_{tr}^{-1}\boldsymbol{\xi}, \quad \boldsymbol{\delta}_q = -(\tilde{\boldsymbol{M}}_{JC}\ddot{\mathbf{q}}_d + \tilde{\boldsymbol{C}}\dot{\mathbf{q}}_d + \tilde{\boldsymbol{\xi}}) \quad (20)$$

Let $\boldsymbol{K}_{Pr}$ and $\boldsymbol{K}_{Dr}$ denote the diagonal matrices with the PD control gains for controlling the motors of the rigid joints, where the components on the diagonal correspond with elastic joints are 0. The tracking control law for the motors of rigid joints is proposed below:

$$\mathbf{u}_q^{tr} = \hat{\boldsymbol{K}}_{tr}^{-1}(\boldsymbol{K}_{Pr}\mathbf{e}_{qd} + \boldsymbol{K}_{Dr}\dot{\mathbf{e}}_{qd} + \hat{\boldsymbol{M}}_I\ddot{\mathbf{q}} + \hat{\boldsymbol{\mu}}_{mr}^{di}\dot{\mathbf{q}}) \quad (21)$$

Substituting (21) into (18) gives:

$$\begin{aligned} &-(\boldsymbol{K}_{tr}\hat{\boldsymbol{K}}_{tr}^{-1}(\boldsymbol{K}_{Dq} + \boldsymbol{K}_{Dr}) + \boldsymbol{C})\dot{\mathbf{e}}_{qd} \\ &- \boldsymbol{K}_{tr}\hat{\boldsymbol{K}}_{tr}^{-1}(\boldsymbol{K}_{Pq} + \boldsymbol{K}_{Pr})\mathbf{e}_{qd} + \boldsymbol{K}_{tr}(\boldsymbol{\delta}_q - \mathbf{u}_q^{ro}) \\ &+ \tilde{\boldsymbol{\tau}}_{elas}^q - \boldsymbol{K}_{tr}\tilde{\boldsymbol{M}}_I\ddot{\mathbf{q}} - \boldsymbol{K}_{tr}\tilde{\boldsymbol{\mu}}_{mr}^{di}\dot{\mathbf{q}} = \boldsymbol{M}_{JC}\ddot{\mathbf{e}}_{qd} \end{aligned} \quad (22)$$

where

$$\tilde{\boldsymbol{M}}_I = \hat{\boldsymbol{K}}_{tr}^{-1}\hat{\boldsymbol{M}}_I - \boldsymbol{K}_{tr}^{-1}\boldsymbol{M}_I, \; \tilde{\boldsymbol{\mu}}_{mr}^{di} = \hat{\boldsymbol{K}}_{tr}^{-1}\hat{\boldsymbol{\mu}}_{mr}^{di} - \boldsymbol{K}_{tr}^{-1}\boldsymbol{\mu}_{mr}^{di} \quad (23)$$

Consider a Lyapunov function as below:

$$V_1 = \frac{1}{2}\mathbf{e}_{qd}^T\boldsymbol{K}_{tr}\hat{\boldsymbol{K}}_{tr}^{-1}(\boldsymbol{K}_{Pq} + \boldsymbol{K}_{Pr})\mathbf{e}_{qd} + \frac{1}{2}\dot{\mathbf{e}}_{qd}^T\boldsymbol{M}_{JC}\dot{\mathbf{e}}_{qd} \quad (24)$$

Taking the time-derivative of the Lyapunov function V_1 and applying the skew symmetry property of the matrix $\dot{\boldsymbol{M}} - 2\boldsymbol{C} = \dot{\boldsymbol{M}}_{JC} - 2\boldsymbol{C}$ yields:

$$\begin{aligned} \dot{V}_1 &= \dot{\mathbf{e}}_{qd}^T\boldsymbol{K}_{tr}\hat{\boldsymbol{K}}_{tr}^{-1}(\boldsymbol{K}_{Pq} + \boldsymbol{K}_{Pr})\mathbf{e}_{qd} \\ &\quad + \frac{1}{2}\dot{\mathbf{e}}_{qd}^T\dot{\boldsymbol{M}}_{JC}\dot{\mathbf{e}}_{qd} + \dot{\mathbf{e}}_{qd}^T\boldsymbol{M}_{JC}\ddot{\mathbf{e}}_{qd} \\ &= \dot{\mathbf{e}}_{qd}^T\boldsymbol{K}_{tr}\hat{\boldsymbol{K}}_{tr}^{-1}(\boldsymbol{K}_{Pq} + \boldsymbol{K}_{Pr})\mathbf{e}_{qd} + \frac{1}{2}\dot{\mathbf{e}}_{qd}^T(\dot{\boldsymbol{M}}_{JC} - 2\boldsymbol{C})\dot{\mathbf{e}}_{qd} \\ &\quad - \dot{\mathbf{e}}_{qd}^T\boldsymbol{K}_{tr}\hat{\boldsymbol{K}}_{tr}^{-1}(\boldsymbol{K}_{Dq} + \boldsymbol{K}_{Dr})\dot{\mathbf{e}}_{qd} \\ &\quad - \dot{\mathbf{e}}_{qd}^T\boldsymbol{K}_{tr}\hat{\boldsymbol{K}}_{tr}^{-1}(\boldsymbol{K}_{Pq} + \boldsymbol{K}_{Pr})\mathbf{e}_{qd} + \dot{\mathbf{e}}_{qd}^T\boldsymbol{K}_{tr}(\boldsymbol{\delta}_q - \mathbf{u}_q^{ro}) \\ &\quad + \dot{\mathbf{e}}_{qd}^T\tilde{\boldsymbol{\tau}}_{elas}^q - \dot{\mathbf{e}}_{qd}^T\boldsymbol{K}_{tr}\tilde{\boldsymbol{M}}_I\ddot{\mathbf{q}} - \dot{\mathbf{e}}_{qd}^T\boldsymbol{K}_{tr}\tilde{\boldsymbol{\mu}}_{mr}^{di}\dot{\mathbf{q}} \\ &= -\dot{\mathbf{e}}_{qd}^T\boldsymbol{K}_{tr}\hat{\boldsymbol{K}}_{tr}^{-1}(\boldsymbol{K}_{Dq} + \boldsymbol{K}_{Dr})\dot{\mathbf{e}}_{qd} + \dot{\mathbf{e}}_{qd}^T\boldsymbol{K}_{tr}(\boldsymbol{\delta}_q - \mathbf{u}_q^{ro}) \\ &\quad + \dot{\mathbf{e}}_{qd}^T\tilde{\boldsymbol{\tau}}_{elas}^q - \dot{\mathbf{e}}_{qd}^T\boldsymbol{K}_{tr}\tilde{\boldsymbol{M}}_I\ddot{\mathbf{q}} - \dot{\mathbf{e}}_{qd}^T\boldsymbol{K}_{tr}\tilde{\boldsymbol{\mu}}_{mr}^{di}\dot{\mathbf{q}} \end{aligned} \quad (25)$$

Let $\boldsymbol{K}_{trr}$ and $\dot{\mathbf{e}}_{qdr}$ denote the diagonal matrix and the vector collecting only components from $\boldsymbol{K}_{tr}$ and $\dot{\mathbf{e}}_{qd}$ corresponding to the rigid joints, respectively. Let $\dot{\boldsymbol{Q}}$ and $\ddot{\boldsymbol{Q}}$ denote the diagonal matrices collecting to their diagonals the components of vectors $\dot{\mathbf{q}}$ and $\ddot{\mathbf{q}}$ corresponding to the rigid joints, respectively. Let $\boldsymbol{\Phi}_1$ and $\boldsymbol{\Phi}_2$ denote vectors collecting the components in the diagonals of $\boldsymbol{\mu}_{mr}^{di}$ and $\boldsymbol{M}_I$ corresponding to the rigid joints, respectively, where:

$$\boldsymbol{\Phi}_1 = \mathrm{diag}(\Phi_{1_1}, ..., \Phi_{1_{N-N_e}}), \;\; \boldsymbol{\Phi}_2 = \mathrm{diag}(\Phi_{2_1}, ..., \Phi_{2_{N-N_e}}) \quad (26)$$

where $\Phi_{1_k} = \mu_{mr_i}^{di}$ and $\Phi_{2_k} = \eta_{m_i}{}^2 I_{mz_i}$ if joint i is the k^{th} rigid joint.

Let $\tilde{\boldsymbol{\Phi}}_1 = \hat{\boldsymbol{\Phi}}_1 - \boldsymbol{\Phi}_1$ and $\tilde{\boldsymbol{\Phi}}_2 = \hat{\boldsymbol{\Phi}}_2 - \boldsymbol{\Phi}_2$ denote the estimation errors. Then $\dot{V}_1$ becomes:

$$\begin{aligned} \dot{V}_1 = &-\dot{\mathbf{e}}_{qd}^T\boldsymbol{K}_{tr}\hat{\boldsymbol{K}}_{tr}^{-1}(\boldsymbol{K}_{Dq} + \boldsymbol{K}_{Dr})\dot{\mathbf{e}}_{qd} + \dot{\mathbf{e}}_{qd}^T\boldsymbol{K}_{tr}(\boldsymbol{\delta}_q - \mathbf{u}_q^{ro}) \\ &+ \dot{\mathbf{e}}_{qd}^T\tilde{\boldsymbol{\tau}}_{elas}^q - \dot{\mathbf{e}}_{qdr}^T\dot{\boldsymbol{Q}}\boldsymbol{K}_{trr}\tilde{\boldsymbol{\Phi}}_1 - \dot{\mathbf{e}}_{qdr}^T\ddot{\boldsymbol{Q}}\boldsymbol{K}_{trr}\tilde{\boldsymbol{\Phi}}_2 \end{aligned} \quad (27)$$

Let $\boldsymbol{\Lambda}_1$ and $\boldsymbol{\Lambda}_2$ denote the diagonal matrices of adaptive coefficients. Consider another Lyapunov function:

$$V_2 = V_1 + \frac{1}{2}\tilde{\boldsymbol{\Phi}}_1^T\boldsymbol{\Lambda}_1^{-1}\boldsymbol{K}_{trr}\tilde{\boldsymbol{\Phi}}_1 + \frac{1}{2}\tilde{\boldsymbol{\Phi}}_2^T\boldsymbol{\Lambda}_2^{-1}\boldsymbol{K}_{trr}\tilde{\boldsymbol{\Phi}}_2 \quad (28)$$

Taking the time-derivative of the Lyapunov function V_2 results in:

$$\begin{aligned} \dot{V}_2 &= \dot{V}_1 + \dot{\tilde{\boldsymbol{\Phi}}}_1^T\boldsymbol{\Lambda}_1^{-1}\boldsymbol{K}_{trr}\tilde{\boldsymbol{\Phi}}_1 + \dot{\tilde{\boldsymbol{\Phi}}}_2^T\boldsymbol{\Lambda}_2^{-1}\boldsymbol{K}_{trr}\tilde{\boldsymbol{\Phi}}_2 \\ &= -\dot{\mathbf{e}}_{qd}^T\boldsymbol{K}_{tr}\hat{\boldsymbol{K}}_{tr}^{-1}(\boldsymbol{K}_{Dq} + \boldsymbol{K}_{Dr})\dot{\mathbf{e}}_{qd} + \dot{\mathbf{e}}_{qd}^T\boldsymbol{K}_{tr}(\boldsymbol{\delta}_q - \mathbf{u}_q^{ro}) \\ &+ \dot{\mathbf{e}}_{qd}^T\tilde{\boldsymbol{\tau}}_{elas}^q + (\dot{\tilde{\boldsymbol{\Phi}}}_1^T\boldsymbol{\Lambda}_1^{-1} - \dot{\mathbf{e}}_{qdr}^T\dot{\boldsymbol{Q}})\boldsymbol{K}_{trr}\tilde{\boldsymbol{\Phi}}_1 \\ &+ (\dot{\tilde{\boldsymbol{\Phi}}}_2^T\boldsymbol{\Lambda}_2^{-1} - \dot{\mathbf{e}}_{qdr}^T\ddot{\boldsymbol{Q}})\boldsymbol{K}_{trr}\tilde{\boldsymbol{\Phi}}_2 \end{aligned} \quad (29)$$

By choosing the adaptive law as:

$$\dot{\hat{\boldsymbol{\Phi}}}_1 = \boldsymbol{\Lambda}_1 \dot{\boldsymbol{Q}} \dot{\mathbf{e}}_{qdr}, \quad \dot{\hat{\boldsymbol{\Phi}}}_2 = \boldsymbol{\Lambda}_2 \ddot{\boldsymbol{Q}} \dot{\mathbf{e}}_{qdr} \tag{30}$$

The derivative $\dot{V}_2$ becomes:

$$\begin{aligned}\dot{V}_2 = & -\dot{\mathbf{e}}_{qd}^T \boldsymbol{K}_{tr} \hat{\boldsymbol{K}}_{tr}^{-1} (\boldsymbol{K}_{Dq} + \boldsymbol{K}_{Dr}) \dot{\mathbf{e}}_{qd} \\ & + \dot{\mathbf{e}}_{qd}^T \boldsymbol{K}_{tr} (\boldsymbol{\delta}_q - \mathbf{u}_q^{ro}) + \dot{\mathbf{e}}_{qd}^T \tilde{\boldsymbol{\tau}}_{elas}^q\end{aligned} \tag{31}$$

Let $\mathbf{q}_e$ and $\mathbf{q}_{d_e}$ denote the vector collecting only components from $\mathbf{q}$ and $\mathbf{q}_d$ corresponding to the elastic joints, respectively. To obtain the robust control parts $\mathbf{u}_q^{ro}$ and $\mathbf{u}_\theta^{ro}$, firstly, the following inequalities are assumed to hold:

$$\|\boldsymbol{K}_{tr} \tilde{\boldsymbol{M}}_{JC}\| = \left\|\boldsymbol{K}_{tr}(\boldsymbol{K}_{tr}^{-1} \boldsymbol{M}_{JC} - \hat{\boldsymbol{K}}_{tr}^{-1} \hat{\boldsymbol{M}}_{JC})\right\| \leqslant M_M \tag{32}$$

$$\|\boldsymbol{K}_{tr} \tilde{\boldsymbol{S}}\| = \left\|\boldsymbol{K}_{tr}(\boldsymbol{K}_{tr}^{-1} \boldsymbol{S} - \hat{\boldsymbol{K}}_{tr}^{-1} \hat{\boldsymbol{S}})\right\| \leqslant S_M^q \tag{33}$$

$$\|\boldsymbol{K}_{tr} \tilde{\boldsymbol{C}}\| = \left\|\boldsymbol{K}_{tr}(\boldsymbol{K}_{tr}^{-1} \boldsymbol{C} - \hat{\boldsymbol{K}}_{tr}^{-1} \hat{\boldsymbol{C}})\right\| \leqslant C_M \tag{34}$$

$$\|\boldsymbol{K}_{tr} \tilde{\boldsymbol{C}}_1\| = \left\|\boldsymbol{K}_{tr}(\boldsymbol{K}_{tr}^{-1} \boldsymbol{C}_1 - \hat{\boldsymbol{K}}_{tr}^{-1} \hat{\boldsymbol{C}}_1)\right\| \leqslant C_{1M} \tag{35}$$

$$\|\boldsymbol{K}_{tr} \tilde{\boldsymbol{G}}\| = \left\|\boldsymbol{K}_{tr}(\boldsymbol{K}_{tr}^{-1} \boldsymbol{G} - \hat{\boldsymbol{K}}_{tr}^{-1} \hat{\boldsymbol{G}})\right\| \leqslant G_M \tag{36}$$

$$\|\boldsymbol{K}_{te} \tilde{\boldsymbol{S}}\| = \left\|\boldsymbol{K}_{te}(\boldsymbol{K}_{te}^{-1} \boldsymbol{S}^T - \hat{\boldsymbol{K}}_{te}^{-1} \hat{\boldsymbol{S}}^T)\right\| \leqslant S_M^\theta \tag{37}$$

$$\|\boldsymbol{K}_{te} \tilde{\boldsymbol{C}}_2\| = \left\|\boldsymbol{K}_{te}(\boldsymbol{K}_{te}^{-1} \boldsymbol{C}_2 - \hat{\boldsymbol{K}}_{te}^{-1} \hat{\boldsymbol{C}}_2)\right\| \leqslant C_{2M} \tag{38}$$

$$\begin{aligned}\|\dot{\mathbf{q}}\| \leqslant Q_{1M}, \|\ddot{\mathbf{q}}\| \leqslant Q_{2M}, \|\dot{\boldsymbol{\theta}}\| \leqslant \Theta_{1M}, \|\ddot{\boldsymbol{\theta}}\| \leqslant \Theta_{2M}, \\ \|\dot{\mathbf{q}}_d\| \leqslant Q_{1DM}, \|\ddot{\mathbf{q}}_d\| \leqslant Q_{2DM}\end{aligned} \tag{39}$$

$$\left\|\boldsymbol{I} - \boldsymbol{K}_{tr} \hat{\boldsymbol{K}}_{tr}^{-1}\right\| \leqslant \alpha < 1, \ \left\|\boldsymbol{I} - \boldsymbol{K}_{te} \hat{\boldsymbol{K}}_{te}^{-1}\right\| \leqslant \beta < 1 \tag{40}$$

$$\begin{aligned}&\left\|\boldsymbol{K} - \hat{\boldsymbol{K}}\right\| \leqslant \left\|\boldsymbol{K}\right\| + \left\|\hat{\boldsymbol{K}}\right\| \leqslant k_M, \\ &\|\boldsymbol{K}_{te} \tilde{\boldsymbol{K}}\| = \left\|\boldsymbol{K}_{te}(\boldsymbol{K}_{te}^{-1} \boldsymbol{K} - \hat{\boldsymbol{K}}_{te}^{-1} \hat{\boldsymbol{K}})\right\| \leqslant K_M, \\ &\left\|\boldsymbol{\theta}_d - \mathbf{q}_{d_e}\right\| \leqslant \Delta_M, \left\|\boldsymbol{\theta} - \mathbf{q}_e\right\| \leqslant \Delta_M\end{aligned} \tag{41}$$

Remark 1: The dynamic matrices are actually functions of trigonometric quantities, and actual joint, motor velocities, and accelerations, as well as desired velocities and accelerations can not be infinity in practice. Thus, inequalities in (32)-(39) are practically feasible. The inequality (40) can be obtained by appropriately choosing the nominated matrices $\hat{\boldsymbol{K}}_{tr}^{-1}$ and $\hat{\boldsymbol{K}}_{te}^{-1}$. Moreover, the stiffness of the springs of elastic joints is not infinite, and the deviation between the motor and joint angular positions has to stay within the elastic ranges of the springs. Therefore, the inequality (41) is also satisfied.

Then:

$$\begin{aligned}\left\|\boldsymbol{K}_{tr} \tilde{\boldsymbol{\xi}}\right\| &= \left\|\boldsymbol{K}_{tr}(\boldsymbol{K}_{tr}^{-1} \boldsymbol{\xi} - \hat{\boldsymbol{K}}_{tr}^{-1} \hat{\boldsymbol{\xi}})\right\| \\ &\leqslant S_M^q \Theta_{2M} + C_{1M} \Theta_{1M} + G_M = \xi_M\end{aligned} \tag{42}$$

$$\begin{aligned}\|\boldsymbol{K}_{tr} \boldsymbol{\delta}_q\| &= \|{-\boldsymbol{K}_{tr}}(\tilde{\boldsymbol{M}}_{JC} \ddot{\mathbf{q}}_d + \tilde{\boldsymbol{C}} \dot{\mathbf{q}}_d + \tilde{\boldsymbol{\xi}})\| \\ &\leqslant M_M Q_{2DM} + C_M Q_{1DM} + \xi_M\end{aligned} \tag{43}$$

$$\begin{aligned}\|\boldsymbol{K}_{te} \boldsymbol{\delta}_\theta\| &= \|{-\boldsymbol{K}_{te}}(\tilde{\boldsymbol{S}} \ddot{\mathbf{q}} + \tilde{\boldsymbol{C}}_2 \dot{\mathbf{q}} + \tilde{\boldsymbol{K}}(\boldsymbol{\theta} - \mathbf{q}_e))\| \\ &\leqslant S_M^\theta Q_{2M} + C_{2M} Q_{1M} + K_M \Delta_M\end{aligned} \tag{44}$$

The discrete robust control part $\mathbf{u}_q^{ro}$ is proposed, with an error threshold E_{qdM}, as below:

$$\mathbf{u}_q^{ro} = \begin{cases} \rho_{r_1} \hat{\boldsymbol{K}}_{tr}^{-1} \dot{\mathbf{e}}_{qd} & \text{if } \|\dot{\mathbf{e}}_{qd}\| \geqslant E_{qdM} > 0 \\ \mathbf{0} & \text{if } \|\dot{\mathbf{e}}_{qd}\| < E_{qdM} \end{cases} \tag{45}$$

When the norm $\|\dot{\mathbf{e}}_{qd}\| < E_{qdM}$, it can be considered that ρ_{r_1} is set to 0.

Consider the last two terms in (31):

$$\begin{aligned}&\dot{\mathbf{e}}_{qd}^T \boldsymbol{K}_{tr} (\boldsymbol{\delta}_q - \mathbf{u}_q^{ro}) + \dot{\mathbf{e}}_{qd}^T \tilde{\boldsymbol{\tau}}_{elas}^q \\ &\leqslant \|\dot{\mathbf{e}}_{qd}\| \|\boldsymbol{K}_{tr} \boldsymbol{\delta}_q\| + \rho_{r_1} \dot{\mathbf{e}}_{qd}^T (\boldsymbol{I} - \boldsymbol{K}_{tr} \hat{\boldsymbol{K}}_{tr}^{-1}) \dot{\mathbf{e}}_{qd} - \rho_{r_1} \dot{\mathbf{e}}_{qd}^T \dot{\mathbf{e}}_{qd} \\ &\quad + \|\dot{\mathbf{e}}_{qd}\| (\|\hat{\boldsymbol{K}}\| \|\boldsymbol{\theta}_d - \mathbf{q}_{d_e}\| + \|\boldsymbol{K}\| \|\boldsymbol{\theta} - \mathbf{q}_e\|) \\ &\leqslant \|\dot{\mathbf{e}}_{qd}\| (M_M Q_{2DM} + C_M Q_{1DM} + \xi_M + k_M \Delta_M) \\ &\quad + \rho_{r_1} \|\dot{\mathbf{e}}_{qd}\| \|\boldsymbol{I} - \boldsymbol{K}_{tr} \hat{\boldsymbol{K}}_{tr}^{-1}\| \|\dot{\mathbf{e}}_{qd}\| - \rho_{r_1} \|\dot{\mathbf{e}}_{qd}\|^2 \\ &\leqslant \|\dot{\mathbf{e}}_{qd}\| (M_M Q_{2DM} + C_M Q_{1DM} + \xi_M + k_M \Delta_M \\ &\qquad + (\alpha - 1) \rho_{r_1} \|\dot{\mathbf{e}}_{qd}\|)\end{aligned} \tag{46}$$

Then, when $\|\dot{\mathbf{e}}_{qd}\| \geqslant E_{qdM} > 0$, choosing the robust control gain such that:

$$\begin{aligned}\rho_{r_1} &\geqslant \frac{M_M Q_{2DM} + C_M Q_{1DM} + \xi_M + k_M \Delta_M}{(1 - \alpha) E_{qdM}} \\ &\geqslant \frac{M_M Q_{2DM} + C_M Q_{1DM} + \xi_M + k_M \Delta_M}{(1 - \alpha) \|\dot{\mathbf{e}}_{qd}\|}\end{aligned} \tag{47}$$

results in $\dot{V}_2 \leqslant 0$. If the error threshold E_{qdM} is choosing such that when $\|\dot{\mathbf{e}}_{qd}\| < E_{qdM}$, we have $\|\dot{\mathbf{e}}_{qd}\| \approx 0$, then $\dot{V}_2 \approx 0$ in this case.

C. Control signals for the motors of the elastic joints

Next, the control signals for the motors of the elastic joints are derived. If joint i is the k^{th} elastic joint, then:

$$\theta_{d_{k,i}} = \frac{1}{\hat{K}_{k,i}} u_{q_i} + q_i \tag{48}$$

The proposed control law for the elastic joint's motor contribution also consists of three parts, similar to the joint dynamics:

$$\mathbf{v}_{ce} = \mathbf{u}_\theta = \mathbf{u}_\theta^{ct} + \mathbf{u}_\theta^{tr} + \mathbf{u}_\theta^{ro} \tag{49}$$

Let $\mathbf{e}_{\theta d} = \boldsymbol{\theta}_d - \boldsymbol{\theta}$ denote the error between the desired and actual joint positions. Consider the computed torque control law:

$$\mathbf{u}_\theta^{ct} = \hat{\boldsymbol{K}}_{te}^{-1} (\hat{\boldsymbol{S}}^T \ddot{\mathbf{q}} + \hat{\boldsymbol{C}}_2 \dot{\mathbf{q}} + \hat{\boldsymbol{K}} (\boldsymbol{\theta}_d - \mathbf{q}_e)) \tag{50}$$

Substituting (50) into the dynamic equation of the elastic joint's motor contribution in (15) gives:

$$\boldsymbol{B} \ddot{\boldsymbol{\theta}} + \boldsymbol{\mu}_{me}^{di} \dot{\boldsymbol{\theta}} = -\boldsymbol{K}_{te} \boldsymbol{\delta}_\theta + \boldsymbol{K}_{te} \hat{\boldsymbol{K}}_{te}^{-1} \hat{\boldsymbol{K}} \mathbf{e}_{\theta d} + \boldsymbol{K}_{te} (\mathbf{u}_\theta^{tr} + \mathbf{u}_\theta^{ro}) \tag{51}$$

where:

$$\tilde{\boldsymbol{S}} = \hat{\boldsymbol{K}}_{te}^{-1} \hat{\boldsymbol{S}}^T - \boldsymbol{K}_{te}^{-1} \boldsymbol{S}^T, \quad \tilde{\boldsymbol{C}} = \hat{\boldsymbol{K}}_{te}^{-1} \hat{\boldsymbol{C}}_2 - \boldsymbol{K}_{te}^{-1} \boldsymbol{C}_2 \tag{52}$$

$$\tilde{\boldsymbol{K}} = \hat{\boldsymbol{K}}_{te}^{-1} \hat{\boldsymbol{K}} - \boldsymbol{K}_{te}^{-1} \boldsymbol{K}, \quad \boldsymbol{\delta}_\theta = -(\tilde{\boldsymbol{S}} \ddot{\mathbf{q}} + \tilde{\boldsymbol{C}}_2 \dot{\mathbf{q}} + \tilde{\boldsymbol{K}} (\boldsymbol{\theta} - \mathbf{q}_e)) \tag{53}$$

Let $\boldsymbol{K}_{Pe}$ and $\boldsymbol{K}_{De}$ denote the diagonal matrices with the PD control gains for controlling the motors of the elastic joints, respectively. The tracking control law for the motors of elastic joints is proposed below:

$$\mathbf{u}_\theta^{tr} = \hat{\boldsymbol{K}}_{te}^{-1}(\boldsymbol{K}_{Pe}\mathbf{e}_{\theta d} + \boldsymbol{K}_{De}\dot{\mathbf{e}}_{\theta d} + \hat{\boldsymbol{B}}\ddot{\theta} + \hat{\boldsymbol{\mu}}_{me}^{di}\dot{\theta}) \tag{54}$$

Substituting (54) into (51) gives:

$$\begin{aligned} &-\boldsymbol{K}_{te}\hat{\boldsymbol{K}}_{te}^{-1}(\hat{\boldsymbol{K}} + \boldsymbol{K}_{Pe})\mathbf{e}_{\theta d} + \boldsymbol{K}_{te}(\boldsymbol{\delta}_\theta - \mathbf{u}_\theta^{ro}) \\ &-\boldsymbol{K}_{te}\tilde{\boldsymbol{B}}\ddot{\theta} - \boldsymbol{K}_{te}\tilde{\boldsymbol{\mu}}_{me}^{di}\dot{\theta} = \boldsymbol{K}_{te}\hat{\boldsymbol{K}}_{te}^{-1}\boldsymbol{K}_{De}\dot{\mathbf{e}}_{\theta d} \end{aligned} \tag{55}$$

Consider a Lyapunov function as below:

$$V_3 = V_2 + \frac{1}{2}\mathbf{e}_{\theta d}^T\boldsymbol{K}_{te}\hat{\boldsymbol{K}}_{te}^{-1}\boldsymbol{K}_{De}\mathbf{e}_{\theta d} \tag{56}$$

Taking the time-derivative of the Lyapunov function V_3 gives:

$$\begin{aligned} \dot{V}_3 &= \dot{V}_2 + \mathbf{e}_{\theta d}^T\boldsymbol{K}_{te}\hat{\boldsymbol{K}}_{te}^{-1}\boldsymbol{K}_{De}\dot{\mathbf{e}}_{\theta d} \\ &= \dot{V}_2 - \mathbf{e}_{\theta d}^T\boldsymbol{K}_{te}\hat{\boldsymbol{K}}_{te}^{-1}(\hat{\boldsymbol{K}} + \boldsymbol{K}_{Pe})\mathbf{e}_{\theta d} + \mathbf{e}_{\theta d}^T\boldsymbol{K}_{te}(\boldsymbol{\delta}_\theta - \mathbf{u}_\theta^{ro}) \\ &\quad - \mathbf{e}_{\theta d}^T\boldsymbol{K}_{te}\tilde{\boldsymbol{B}}\ddot{\theta} - \mathbf{e}_{\theta d}^T\boldsymbol{K}_{te}\tilde{\boldsymbol{\mu}}_{me}^{di}\dot{\theta} \end{aligned} \tag{57}$$

Let $\dot{\boldsymbol{\Theta}}$ and $\ddot{\boldsymbol{\Theta}}$ denote the diagonal matrices collecting to their diagonals the components of vectors $\dot{\theta}$ and $\ddot{\theta}$, respectively. Let $\boldsymbol{\Phi}_3$ and $\boldsymbol{\Phi}_4$ denote vectors collecting the components in the diagonals of $\boldsymbol{\mu}_{me}^{di}$ and $\boldsymbol{B}$, respectively, where:

$$\boldsymbol{\Phi}_3 = \text{diag}(\Phi_{3_1}, ..., \Phi_{3_{N_e}}), \quad \boldsymbol{\Phi}_4 = \text{diag}(\Phi_{4_1}, ..., \Phi_{4_{N_e}}) \tag{58}$$

where $\Phi_{3_k} = \mu_{me_k}^{di}$ and $\Phi_{4_k} = {\eta_{m_i}}^2 I_{mz_i}$ if joint i is the k^{th} elastic joint.

Let $\tilde{\boldsymbol{\Phi}}_3 = \hat{\boldsymbol{\Phi}}_3 - \boldsymbol{\Phi}_3$ and $\tilde{\boldsymbol{\Phi}}_4 = \hat{\boldsymbol{\Phi}}_4 - \boldsymbol{\Phi}_4$ denote the estimation errors. Then $\dot{V}_3$ becomes:

$$\begin{aligned} \dot{V}_3 &= \dot{V}_2 - \mathbf{e}_{\theta d}^T\boldsymbol{K}_{te}\hat{\boldsymbol{K}}_{te}^{-1}(\hat{\boldsymbol{K}} + \boldsymbol{K}_{Pe})\mathbf{e}_{\theta d} + \mathbf{e}_{\theta d}^T\boldsymbol{K}_{te}(\boldsymbol{\delta}_\theta - \mathbf{u}_\theta^{ro}) \\ &\quad - \mathbf{e}_{\theta d}^T\dot{\boldsymbol{\Theta}}\boldsymbol{K}_{te}\tilde{\boldsymbol{\Phi}}_3 - \mathbf{e}_{\theta d}^T\ddot{\boldsymbol{\Theta}}\boldsymbol{K}_{te}\tilde{\boldsymbol{\Phi}}_4 \end{aligned} \tag{59}$$

Let $\boldsymbol{\Lambda}_3$ and $\boldsymbol{\Lambda}_4$ denote the diagonal matrices of adaptive coefficients. Consider a Lyapunov function as below:

$$V_4 = V_3 + \frac{1}{2}\tilde{\boldsymbol{\Phi}}_3^T\boldsymbol{\Lambda}_3^{-1}\boldsymbol{K}_{te}\tilde{\boldsymbol{\Phi}}_3 + \frac{1}{2}\tilde{\boldsymbol{\Phi}}_4^T\boldsymbol{\Lambda}_4^{-1}\boldsymbol{K}_{te}\tilde{\boldsymbol{\Phi}}_4 \tag{60}$$

Taking the time-derivative of V_4 yields:

$$\begin{aligned} \dot{V}_4 &= \dot{V}_3 + \dot{\tilde{\boldsymbol{\Phi}}}_3^T\boldsymbol{\Lambda}_3^{-1}\boldsymbol{K}_{te}\tilde{\boldsymbol{\Phi}}_3 + \dot{\tilde{\boldsymbol{\Phi}}}_4^T\boldsymbol{\Lambda}_4^{-1}\boldsymbol{K}_{te}\tilde{\boldsymbol{\Phi}}_4 \\ &= \dot{V}_2 - \mathbf{e}_{\theta d}^T\boldsymbol{K}_{te}\hat{\boldsymbol{K}}_{te}^{-1}(\hat{\boldsymbol{K}} + \boldsymbol{K}_{Pe})\mathbf{e}_{\theta d} + \mathbf{e}_{\theta d}^T\boldsymbol{K}_{te}(\boldsymbol{\delta}_\theta - \mathbf{u}_\theta^{ro}) \\ &+ (\dot{\tilde{\boldsymbol{\Phi}}}_3^T\boldsymbol{\Lambda}_3^{-1} - \mathbf{e}_{\theta d}^T\dot{\boldsymbol{\Theta}})\boldsymbol{K}_{te}\tilde{\boldsymbol{\Phi}}_3 + (\dot{\tilde{\boldsymbol{\Phi}}}_4^T\boldsymbol{\Lambda}_4^{-1} - \mathbf{e}_{\theta d}^T\ddot{\boldsymbol{\Theta}})\boldsymbol{K}_{te}\tilde{\boldsymbol{\Phi}}_4 \end{aligned} \tag{61}$$

By choosing the adaptive law as:

$$\dot{\tilde{\boldsymbol{\Phi}}}_3 = \boldsymbol{\Lambda}_3\dot{\boldsymbol{\Theta}}\mathbf{e}_{\theta d}, \quad \dot{\tilde{\boldsymbol{\Phi}}}_4 = \boldsymbol{\Lambda}_4\ddot{\boldsymbol{\Theta}}\mathbf{e}_{\theta d} \tag{62}$$

The derivative $\dot{V}_4$ becomes:

$$\dot{V}_4 = \dot{V}_2 - \mathbf{e}_{\theta d}^T\boldsymbol{K}_{te}\hat{\boldsymbol{K}}_{te}^{-1}(\hat{\boldsymbol{K}} + \boldsymbol{K}_{Pe})\mathbf{e}_{\theta d} + \mathbf{e}_{\theta d}^T\boldsymbol{K}_{te}(\boldsymbol{\delta}_\theta - \mathbf{u}_\theta^{ro}) \tag{63}$$

The discrete robust control part $\mathbf{u}_\theta^{ro}$ is proposed, with an error threshold $E_{\theta dM}$, as below:

$$\mathbf{u}_\theta^{ro} = \begin{cases} \rho_{r_2}\hat{\boldsymbol{K}}_{te}^{-1}\mathbf{e}_{\theta d} & \text{if } \|\mathbf{e}_{\theta d}\| \geqslant E_{\theta dM} > 0 \\ \mathbf{0} & \text{if } \|\mathbf{e}_{\theta d}\| < E_{\theta dM} \end{cases} \tag{64}$$

TABLE I

DYNAMIC PARAMETERS OF THE JOINTS

	link 1	link 2
mass(kg)	2.5	1.5
inertia (kg.m^2)	$\begin{bmatrix} 0.4 & 0 & 0 \\ 0 & 0.5 & 0 \\ 0 & 0 & 0.4 \end{bmatrix}$	$\begin{bmatrix} 0.35 & 0.15 & 0.1 \\ 0.15 & 0.4 & 0.2 \\ 0.1 & 0.2 & 0.3 \end{bmatrix}$
	link 3	link 4
mass(kg)	1.0	1.5
inertia (kg.m^2)	$\begin{bmatrix} 0.3 & 0.15 & 0.13 \\ 0.15 & 0.25 & 0.2 \\ 0.13 & 0.2 & 0.25 \end{bmatrix}$	$\begin{bmatrix} 0.2 & 0.18 & 0.15 \\ 0.18 & 0.21 & 0.16 \\ 0.15 & 0.16 & 0.23 \end{bmatrix}$
	link 5	link 6
mass(kg)	0.5	0.5
inertia (kg.m^2)	$\begin{bmatrix} 0.1 & 0.08 & 0.07 \\ 0.08 & 0.09 & 0.08 \\ 0.07 & 0.08 & 0.09 \end{bmatrix}$	$\begin{bmatrix} 0.1 & 0.04 & 0.05 \\ 0.04 & 0.07 & 0.04 \\ 0.05 & 0.04 & 0.06 \end{bmatrix}$

TABLE II

DYNAMIC PARAMETERS OF THE MOTORS

motor	inertia (kg.m^2)	mass (kg)	gear ratio	R_a (Ohm)	K_τ (Nm/A)	K_{emf} (V/m/s)
1-3	diag(6,6,4) $*10^{-3}$	1.0	50	0.01	0.01	0.0001
4	diag(4,4,3) $*10^{-3}$	0.8	60	0.01	0.008	0.0001
5-6	diag(2,2,2) $*10^{-3}$	0.6	80	0.01	0.002	0.0001

Consider the last term in (63):

$$\begin{aligned} &\mathbf{e}_{\theta d}^T\boldsymbol{K}_{te}(\boldsymbol{\delta}_\theta - \mathbf{u}_\theta^{ro}) \\ &\leqslant \|\mathbf{e}_{\theta d}\|\|\boldsymbol{K}_{te}\boldsymbol{\delta}_\theta\| + \rho_{r_2}\mathbf{e}_{\theta d}^T(\boldsymbol{I} - \boldsymbol{K}_{te}\hat{\boldsymbol{K}}_{te}^{-1})\mathbf{e}_{\theta d} - \rho_{r_2}\mathbf{e}_{\theta d}^T\mathbf{e}_{\theta d} \\ &\leqslant \|\mathbf{e}_{\theta d}\|(S_M^\theta Q_{2M} + C_{2M}Q_{1M} + K_M\Delta_M) \\ &\quad + \rho_{r_2}\|\mathbf{e}_{\theta d}\|\|\boldsymbol{I} - \boldsymbol{K}_{te}\hat{\boldsymbol{K}}_{te}^{-1}\|\|\mathbf{e}_{\theta d}\| - \rho_{r_2}\|\mathbf{e}_{\theta d}\|^2 \\ &\leqslant \|\mathbf{e}_{\theta d}\|(S_M^\theta Q_{2M} + C_{2M}Q_{1M} + K_M\Delta_M \\ &\qquad + (\beta - 1)\rho_{r_2}\|\mathbf{e}_{\theta d}\|) \end{aligned} \tag{65}$$

Finally, when $\|\mathbf{e}_{\theta d}\| \geqslant E_{\theta dM} > 0$, choosing the robust control gain such that:

$$\begin{aligned} \rho_{r_2} &\geqslant \frac{S_M^\theta Q_{2M} + C_{2M}Q_{1M} + K_M\Delta_M}{(1-\beta)E_{\theta dM}} \\ &\geqslant \frac{S_M^\theta Q_{2M} + C_{2M}Q_{1M} + K_M\Delta_M}{(1-\beta)\|\mathbf{e}_{\theta d}\|} \end{aligned} \tag{66}$$

gives $\dot{V}_4 \leqslant 0$. If the error threshold $E_{\theta dM}$ is choosing such that when $\|\mathbf{e}_{\theta d}\| < E_{\theta dM}$, we have $\|\mathbf{e}_{\theta d}\| \approx 0$, then $\dot{V}_4 \approx 0$ in this case. Therefore, the system is stable.

IV. SIMULATION

The performance of the proposed robust-adaptive two-loop control algorithm for robots with mixed rigid-elastic joints against parameter uncertainties is verified through simulations. The robot has six degrees of freedom (DOFs), as illustrated in Figure 1, where the first three joints are rigid and the last three are elastic. The stiffness coefficients

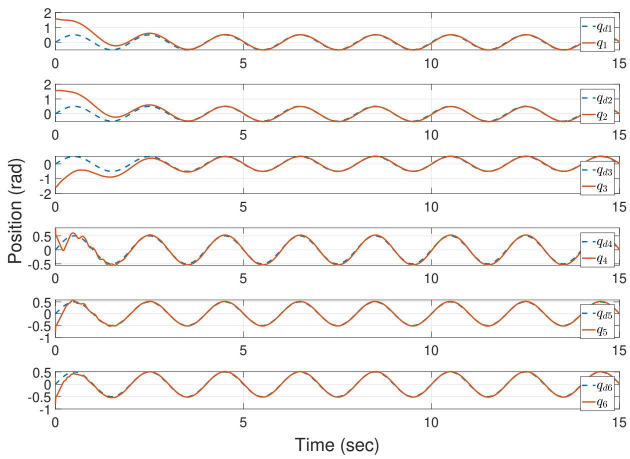

Fig. 3. Angular positions of the joints. The blue line and the red solid line show the desired and actual position of the joints, respectively.

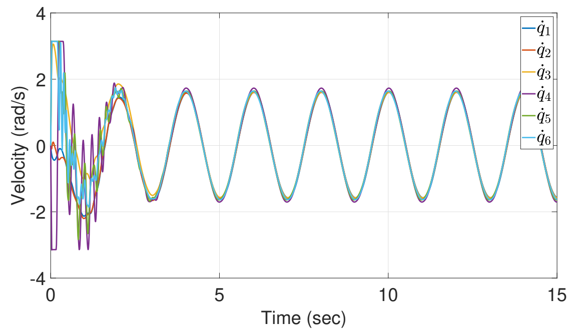

Fig. 4. Angular velocities of the joints.

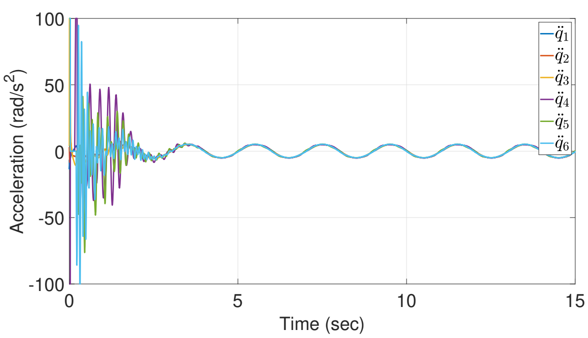

Fig. 5. Angular accelerations of the joints.

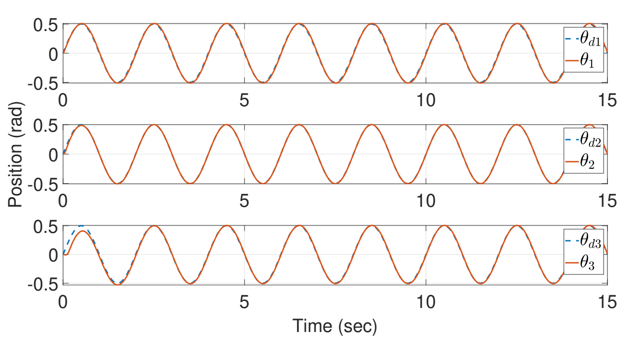

Fig. 6. Angular position of the motor. The blue dashed line and the red solid line show the desired and actual position of the motor, respectively.

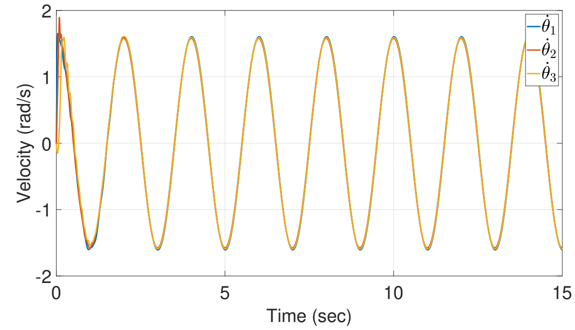

Fig. 7. Angular velocity of the motor.

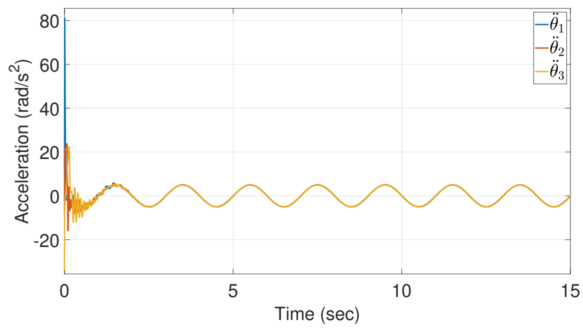

Fig. 8. Angular acceleration of the motor.

of the springs of elastic joints are 250, 200, and 200 (N/m), respectively. Table I and Table II list the dynamic parameters of the joints and motors of the simulated robot, respectively. To simulate the uncertainties, the dynamic parameters used in the algorithm will be randomly scaled by a factor in the range $[0.7\ 1.3]$. This means that the dynamic parameter set used to calculate the dynamics of the robot and the one used in the algorithm are not identical. The desired positions of the joints are sinusoidal functions of the form $0.5\sin(\pi t)$ and the robot is simulated for 15 seconds. The initial positions of the joints are:

$$[\frac{\pi}{2}\ \ \frac{\pi}{2}\ \ \frac{-\pi}{2}\ \ \frac{\pi}{4}\ \ \frac{-\pi}{4}\ \ \frac{-\pi}{4}]^T(\text{rad}) \tag{67}$$

Further, to avoid instability due to overestimation of the adaptive control, the parameters in $\mathbf{\Phi}_1$ and $\mathbf{\Phi}_3$ are limited within the range of $[10^{-5}\ \ 0.5]$ and the

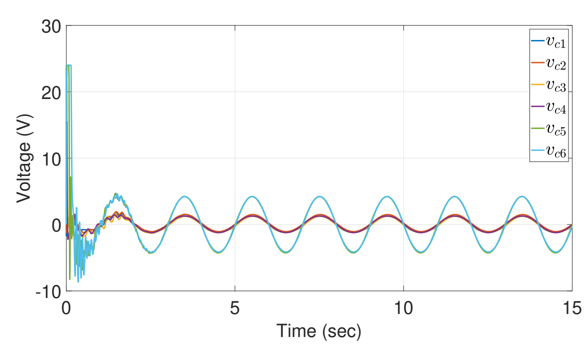

Fig. 9. Control voltage of the motor. The spike of the control voltage at the beginning is due to the large initial error.

parameters in $\mathbf{\Phi}_2$ and $\mathbf{\Phi}_4$ are limited within the range of $[0.9\ 15]$. Moreover, the dead-zone technique is also adopted for the adaptive controller, where the dead-zone for the 1-norm of the errors $||\mathbf{e}_{qdr}||_1$ and $||\mathbf{e}_{\theta d}||_1$ is $[-0.174533\ 0.174533]$ (rad) ($\approx\ \pm 10°$). The control gains are chosen as: $\boldsymbol{K}_{Pq}$=diag(150,150,150,100,100,100), $\boldsymbol{K}_{Dq}$=diag(20,20,20,50,50,50), $\boldsymbol{K}_{Pr}$=diag(30,30,30,0,0,0), $\boldsymbol{K}_{Dr}$=diag(10,10,10,0,0,0), $\boldsymbol{K}_{Pe}$=diag(30,30,30), and $\boldsymbol{K}_{De}$=diag(160,160,160). The last element of the matrix $\hat{\boldsymbol{K}}_{tr}^{-1}$, that is the one corresponding to the elastic joint, is chosen as 0.001 instead of 1. This setup is to reduce the oscillation of the elastic joints. The robust gains are chosen as: ρ_{r_1}=150, and ρ_{r_2}=50. The controller is run every 1 ms.

The angular positions, velocities, and accelerations of the joints are shown in Figures 3, 4, and 5, respectively. The root mean square errors between the desired and actual angular positions for 15 seconds of simulation time of joints are 0.57245, 0.57371, 0.61472, 0.5335, 0.52518, and 0.52601 rad, respectively. The velocity and acceleration of the elastic joint fluctuate while the controller is attempting to keep the tracking error as small as possible. To reduce this fluctuation, either the stiffness coefficients of the springs are reduced or the tracking control gains are reduced. In both ways, the tracking error will increase.

The angular positions, velocities, and accelerations of the motors of elastic joints are shown in Figures 6, 7, and 8, respectively. The tracking error is relatively small. The motor voltages are shown in Figure 9. The control voltages for rigid joints have higher amplitudes than those for elastic joints. This is because motors in elastic joints must work harder to minimise fluctuations in motor outputs and, consequently, in joint angular positions.

V. CONCLUSIONS

This paper proposed a robust-adaptive two-loop control algorithm to manipulate robots with mixed rigid-elastic joints with uncertainties in system parameters. In the outer loop, a robust control algorithm is presented to handle the uncertainties in the dynamic parameters of the joint dynamics, and an adaptive controller manages the rigid joints. In the inner loop, another robust control algorithm handles uncertainties in the elastic joint's motor contribution, complemented by a similar adaptive controller for the elastic joints' motors. Lyapunov's stability theory ensures system stability. The algorithm effectively handles fast-changing disturbances with high-gain robust controllers and computed torque controllers, leaving adaptive controllers to manage slow-changing uncertainties. Simulations demonstrate the algorithm's efficiency in controlling a six-DOF robot with three rigid and three elastic joints. Future work will implement and verify the algorithm on a real mechanical robot with mixed joint types. The accelerations of the joints and motors are used in the design of the control algorithm. Obtaining high-quality, low-noise acceleration measurements might be difficult on real hardware. Therefore, high-resolution encoders and high sampling rates are required when implementing the algorithm on real hardware to obtain good-quality acceleration measurements. Furthermore, the behaviour of the whole system when interacting with the surroundings will also be considered [21]. Moreover, the possibility of comparing the performance of the proposed algorithm with existing control approaches, such as [4], [5], will be investigated.

REFERENCES

[1] B. Siciliano, O. Khatib, and T. Kröger, *Springer handbook of robotics*. Springer, 2008, vol. 200.

[2] C. Ott, *Cartesian impedance control of redundant and flexible-joint robots*. Springer, 2008.

[3] H. M. Tuan, F. Sanfilippo, and N. V. Hao, "A novel adaptive sliding mode controller for a 2-dof elastic robotic arm," *Robotics*, vol. 11, no. 2, p. 47, 2022.

[4] A. De Luca and R. Farina, "Dynamic properties and nonlinear control of robots with mixed rigid/elastic joints," in *Proc. World Automation Congress, 2004.*, vol. 15. IEEE, 2004, pp. 97–104.

[5] A. De Luca, "Decoupling and feedback linearization of robots with mixed rigid/elastic joints," *International Journal of Robust and Nonlinear Control: IFAC-Affiliated Journal*, vol. 8, no. 11, pp. 965–977, 1998.

[6] M. W. Spong, "Modeling and control of elastic joint robots," *Journal of Dynamic Systems, Measurement, and Control*, 1987.

[7] J. S. Yeon and J. H. Park, "Practical robust control for flexible joint robot manipulators," in *Proc. of the IEEE International Conference on Robotics and Automation*, 2008, pp. 3377–3382.

[8] K. Rsetam, Z. Cao, and Z. Man, "Design of robust terminal sliding mode control for underactuated flexible joint robot," *IEEE Transactions on Systems, Man, and Cybernetics: Systems*, vol. 52, no. 7, pp. 4272–4285, 2021.

[9] X. Cheng, H. Liu, and W. Lu, "Chattering-suppressed sliding mode control for flexible-joint robot manipulators," in *Actuators*, vol. 10, no. 11. MDPI, 2021, p. 288.

[10] S. Han, H. Wang, and H. Yu, "Nonlinear disturbance observer-based robust motion control for multi-joint series elastic actuator-driven robots," in *Proc. of the IEEE International Conference on Robotics and Automation (ICRA)*, 2021, pp. 10 469–10 475.

[11] B. Zhan, M. Jin, and J. Liu, "Extended-state-observer-based adaptive control of flexible-joint space manipulators with system uncertainties," *Advances in Space Research*, vol. 69, no. 8, pp. 3088–3102, 2022.

[12] S. Chen and J. T. Wen, "Adaptive neural trajectory tracking control for flexible-joint robots with online learning," in *Proc. of the IEEE International Conference on Robotics and Automation (ICRA)*, 2020, pp. 2358–2364.

[13] S. Zaare and M. R. Soltanpour, "Adaptive fuzzy global coupled nonsingular fast terminal sliding mode control of n-rigid-link elastic-joint robot manipulators in presence of uncertainties," *Mechanical Systems and Signal Processing*, vol. 163, p. 108165, 2022.

[14] K. Lu, S. Han, J. Yang, and H. Yu, "Inverse optimal adaptive tracking control of robotic manipulators driven by compliant actuators," *IEEE Transactions on Industrial Electronics*, 2023.

[15] T. M. Hua, F. Sanfilippo, and H. Nguyen Vinh, "Modelling and control of a 2-DOF robot arm with elastic actuators for safe human-robot interaction," *Frontiers in Robotics and AI*, vol. 8, p. 223, 2021.

[16] W.-H. Zhu and J. De Schutter, "Adaptive control of mixed rigid/flexible joint robot manipulators based on virtual decomposition," *IEEE Transactions on Robotics and Automation*, vol. 15, no. 2, pp. 310–317, 1999.

[17] W.-H. Zhu and J. De Schutter, "Virtual decomposition based motion/force control of a kuka361 industrial manipulator," *IFAC Proc. Volumes*, vol. 35, no. 1, pp. 241–246, 2002.

[18] B. Siciliano, L. Sciavicco, L. Villani, and G. Oriolo, *Robotics: Modelling, Planning and Control*. Springer, 2009.

[19] P. A. Ioannou and J. Sun, *Robust adaptive control*. Courier Corporation, 2012.

[20] M. R. Soltanpour, M. Moattari *et al.*, "Voltage based sliding mode control of flexible joint robot manipulators in presence of uncertainties," *Robotics and Autonomous Systems*, vol. 118, pp. 204–219, 2019.

[21] E. F. Langås, M. H. Zafar, S. O. Nyberg, and F. Sanfilippo, "Human trajectory simulation in industrial settings using the ornstein-uhlenbeck process and deep learning based classification," in *Proc. of the 10th IEEE International Conference on Automation, Robotics and Applications (ICARA)*, 2024, pp. 427–432.